

Extracting semiconductor band gap zero-point corrections from experimental data

Bartomeu Monserrat,^{*} G. J. Conduit, and R. J. Needs

TCM Group, Cavendish Laboratory, University of Cambridge, J. J. Thomson Avenue, Cambridge CB3 0HE, United Kingdom

(Received 15 August 2013; published 12 November 2014)

We describe an improved method for extracting semiconductor band gap zero-point corrections from experimental data. We propose two extrapolation schemes and use first-principles calculations to show that they are up to an order of magnitude more accurate than existing schemes. We apply our schemes to diamond, extracting a value of the zero-point correction of -0.41 eV, in better agreement with first-principles results than previous estimates. Finally, we consider the low-temperature limit of the class of observables that includes the electronic band gap, obtaining a T^4 dependence in three dimensions, T^2 in two dimensions, and $T^{3/2}$ in one dimension.

DOI: [10.1103/PhysRevB.90.184302](https://doi.org/10.1103/PhysRevB.90.184302)

PACS number(s): 63.20.dk, 71.38.-k, 71.15.Mb

I. INTRODUCTION

Atomic vibrations have a substantial impact on the properties of solids, for example for their thermodynamic stability, equilibrium volume, or optical and electronic responses. The quantum nuclear zero-point (ZP) vibrational motion is particularly important for light atoms, although it is not straightforward to measure its effects because static lattice structures are not physically realizable. The effects of finite temperatures on directly measurable key properties, such as the electronic band gaps and equilibrium volumes, are significant and are driven mainly by the atomic vibrations. The importance of considering the vibrational state of a solid was evident from the early days of quantum theory, motivating the Einstein [1] and Debye [2] models for the specific heat. The advent of first-principles calculations has revolutionized the analysis of vibrations in solids [3,4], taking the initial qualitative models to the arena of quantitative predictive science.

The temperature dependence of band gaps in solids has long been a focus for experimentalists [5–12], and theoretical calculations were pioneered by Allen, Heine, and Cardona [13–15]. There is increasing interest in the use of first-principles calculations for studying the temperature dependence of band gaps [16–31], which makes the availability of accurate experimental data highly desirable in order to validate these methods. In this paper we study two aspects of band gaps: (i) the extraction from experimental data of the ZP correction to the band gap, a quantity readily available in theoretical calculations, and (ii) the power-law dependence of the value of the band gap on temperature as $T \rightarrow 0$, a quantity that is difficult to access with first-principles methods.

ZP corrections to the band gap are not easily accessible from experiment. A number of schemes have been proposed for extracting these corrections from temperature-dependent experimental data [11,32–35]. In this paper we use first-principles results for the temperature dependence of the band gap of diamond and lithium hydride to assess the validity of a range of extrapolation schemes. We show that currently used schemes result in significant inaccuracies, and propose two extrapolation schemes that improve the accuracy of the results by up to an order of magnitude.

In recent years there has been a surge of interest in low-dimensional systems such as graphene and carbon nanotubes. The asymptotic behavior of the band gap as $T \rightarrow 0$ is difficult to calculate using first-principles methods. In this work we extend the three-dimensional T^4 asymptotic limit of the temperature dependence of the band gap as $T \rightarrow 0$ [36] to low-dimensional systems. We find that two-dimensional systems obey a T^2 power law, and one-dimensional systems follow a $T^{3/2}$ power law, both dominated by the quadratic acoustic branches.

In Sec. II we outline the harmonic theory of the temperature dependence of band gaps. In Sec. III we propose two models for use within an extrapolation scheme for obtaining the ZP correction to band gaps. In Sec. IV we describe the asymptotic behavior of band gaps at low temperatures. We summarize our findings in Sec. V.

II. VIBRATIONAL EXPECTATION VALUE

We first describe the general framework for calculating the expectation value of an observable \hat{O} that depends on the vibrational state of the solid. We are interested in the “ZP correction” to a general physical observable, defined as the difference between the value of the observable when the atoms are assumed to be static at their equilibrium positions, and when the quantum mechanical motion at $T = 0$ K is included. We will focus on the ZP correction to the electronic band gap, which can be used to gauge the strength of the electron-phonon coupling.

We model a solid of N atoms by a supercell subject to periodic boundary conditions. The vibrational motion of the atoms can be described within the harmonic approximation in terms of $3N$ phonon coordinates $\{q_{n\mathbf{k}}\}$, where n is the branch index and \mathbf{k} is a reciprocal space vector within the first Brillouin zone (BZ). In terms of phonon coordinates, the vibrational Hamiltonian $\hat{\mathcal{H}}$ reads

$$\hat{\mathcal{H}} = \sum_{n,\mathbf{k}} \left(-\frac{1}{2} \frac{\partial^2}{\partial q_{n\mathbf{k}}^2} + \frac{1}{2} \omega_{n\mathbf{k}}^2 q_{n\mathbf{k}}^2 \right), \quad (1)$$

where the $\omega_{n\mathbf{k}}$ are phonon frequencies. The energy associated with a phonon mode (n,\mathbf{k}) in state m is $E_{n\mathbf{k};m} = \omega_{n\mathbf{k}}(m + 1/2)$, and the corresponding state is $|\phi_m(q_{n\mathbf{k}})\rangle$. We label the vibrational state of the solid by the $3N$ -dimensional

^{*}bm418@cam.ac.uk

vector \mathbf{M} , whose element $M_{n\mathbf{k}}$ labels the state of phonon (n, \mathbf{k}) . All equations are given in Hartree atomic units, $\hbar = |e| = m_e = 4\pi\epsilon_0 = 1$.

Let \mathbf{q} be a collective vibrational coordinate with elements $q_{n\mathbf{k}}$. The expectation value at inverse temperature $\beta = 1/k_B T$ with respect to the vibrational state $|\Phi_{\mathbf{M}}\rangle = \prod_{n,\mathbf{k}} |\phi_{M_{n\mathbf{k}}}(q_{n\mathbf{k}})\rangle$ is

$$\langle \hat{O} \rangle = \frac{1}{\mathcal{Z}} \sum_{\mathbf{M}} \langle \Phi_{\mathbf{M}}(\mathbf{q}) | \hat{O}(\mathbf{q}) | \Phi_{\mathbf{M}}(\mathbf{q}) \rangle e^{-\beta E_{\mathbf{M}}}, \quad (2)$$

where $\mathcal{Z} = \sum_{\mathbf{M}} e^{-\beta E_{\mathbf{M}}}$ is the partition function.

This expectation value has been evaluated directly by Monte Carlo sampling [23,26,37], path-integral methods [38], or by using a perturbative expansion, which gives the so-called Allen-Heine-Cardona (AHC) theory. The perturbative solution can be obtained by expanding the operator as

$$\hat{O}(\mathbf{q}) = \sum_{n,\mathbf{k}} a_{n\mathbf{k}} q_{n\mathbf{k}}^2, \quad (3)$$

where $a_{n\mathbf{k}}$ are the coupling constants. This expression for the observable \hat{O} in Eq. (2) leads to [39]

$$\langle \hat{O} \rangle = \sum_{n,\mathbf{k}} \frac{a_{n\mathbf{k}}}{2\omega_{n\mathbf{k}}} [1 + 2n_B(\omega_{n\mathbf{k}})], \quad (4)$$

where $n_B(\omega) = (e^{\beta\omega} - 1)^{-1}$ is a Bose-Einstein (BE) factor, and the expression in Eq. (4) is accurate to fourth order in the vibrational normal mode amplitude $q_{n\mathbf{k}}$. This formulation is used in first-principles calculations, and includes the so-called nondiagonal Debye-Waller term, which is neglected in some formulations of AHC theory [19]. We note here that the high-temperature limit of Eq. (4) is

$$\langle \hat{O} \rangle \xrightarrow{\beta \ll 1} \left(\sum_{n,\mathbf{k}} \frac{a_{n\mathbf{k}}}{\omega_{n\mathbf{k}}^2} \right) \beta^{-1}. \quad (5)$$

At high temperatures the band gap therefore varies linearly with temperature.

III. DETERMINING THE ZERO-POINT CORRECTION

The experimental characterization of the vibrational state of a solid is important for understanding many physical phenomena. The ZP correction to an observable is a direct measure of the coupling between the observable and the phonons. However, this quantity cannot be measured directly in experiments because it relates to a physically unobservable state without nuclear vibrations. With the first-principles method described in Ref. [22], we first expose the shortcomings of the different models used to extract the ZP correction from experimental data, and second propose two schemes and assess their accuracy.

From Eq. (4), the ZP correction to an observable \hat{O} is given by

$$\langle \hat{O} \rangle_{\text{ZP}} = \frac{1}{2} \sum_{n,\mathbf{k}} \frac{a_{n\mathbf{k}}}{\omega_{n\mathbf{k}}}, \quad (6)$$

and can be extracted from the extrapolation to zero temperature from the high-temperature limit $\beta \ll 1/\omega$ [39]. In practical applications of the extrapolation scheme, there are rarely

TABLE I. Analytic models for the temperature dependence of phonon-renormalized quantities.

Model	$F(T, \mathbf{A})$
Varshni	$A_0 + \frac{A_1 T^2}{A_2 + T}$
Pässler	$A_0 + \frac{A_1 A_2}{2} \left\{ \left[1 + \left(\frac{2T}{A_2} \right)^{A_3} \right]^{1/A_3} + 1 \right\}$
BE	$\frac{A_0}{e^{\bar{\omega}/k_B T} - 1}$
Double BE	$\frac{A_0}{e^{\bar{\omega}_0/k_B T} - 1} + \frac{A_1}{e^{\bar{\omega}_1/k_B T} - 1}$
Phonon dispersion	$\frac{A_0}{e^{\bar{\omega}/k_B T} - 1} + \frac{e^{\bar{\omega}/k_B T} A_1}{k_B T (e^{\bar{\omega}/k_B T} - 1)^2} + \frac{e^{\bar{\omega}/k_B T} (1 + e^{\bar{\omega}/k_B T}) A_2}{2(k_B T)^2 (e^{\bar{\omega}/k_B T} - 1)^3} + \dots$
Two step	$\frac{A_0}{e^{\bar{\omega}/k_B T} - 1}$ $\omega(T_{\max}) = p_0 + \frac{p_1 p_0^2}{k_B T_{\max} \ln(p_0/k_B T_{\max})}$ $A(T_{\max}) = p_2 \left(p_0 + \frac{p_1 p_0^2}{k_B T_{\max}} \right)$

enough experimental data to approach the high-temperature limit. One can construct an analytic model $F(T, \mathbf{A})$ for the T dependence of the observable over the entire temperature range, fitted using parameters \mathbf{A} . This analytical model is then used in the extrapolation. Using first-principles data generated by the method presented in Ref. [22] that describes the temperature dependence of band gaps, we assess the different models $F(T, \mathbf{A})$. We propose two schemes and test them against previous models and obtain a significant improvement in the accuracy of the extrapolated ZP correction. The models considered for $F(T, \mathbf{A})$ are reported in Table I. We note that the older models were not developed specifically for the ZP extrapolation, but instead to accurately reproduce the experimental data, which is usually available only at low temperatures. This might explain some of the failures in their application to extracting accurate ZP corrections.

A widely used model proposed by Varshni [32] reproduces the high-temperature linear asymptote, but incorrectly assumes a T^2 dependence as $T \rightarrow 0$. Pässler [35] proposed a more complicated expression, which describes the low-temperature behavior by a fitting parameter that in principle could recover the low-temperature T^4 limit (see Sec. IV below and Ref. [36]). However, the low-temperature asymptote has little impact on the high-temperature limit or the ZP correction because the cross-over between a power law and the exponential dependence of Eq. (4) occurs at very low temperatures (below 4 K for silicon [36]) and, moreover, the acoustic phonons that dominate in this regime have a low density of states. This motivates neglecting the low-temperature T^4 power law and instead focusing on the higher energy phonon branches that can be described by the Einstein approximation. This leads to a functional form consisting of a single BE oscillator [34], which amounts to assuming a dispersionless phonon spectrum. As the correct expression for the observable in Eq. (4) consists of a sum over many BE oscillators, a straightforward extension of the single BE oscillator model is to include a second oscillator [33]. For systems with nonmonotonic temperature-dependent gaps, characterized by more than one Einstein frequency, the use of more than one BE oscillator is essential [11] (see Sec. III B 2 below).

A. Two linear extrapolation schemes

The BE oscillator model may fail to recover the ZP correction unless data are available up to high temperatures $k_B T \gtrsim \omega$. This motivates us to propose two methods based on a single BE oscillator fit [34],

$$F(T, \mathbf{A}) = \frac{A_0}{e^{\omega/k_B T} - 1}, \quad (7)$$

where $\mathbf{A} = (A_0, \omega)$. We show that our two approaches recover the correct ZP correction even with data restricted to low temperatures.

1. Phonon dispersion method

We start from Eq. (4), rewrite the phonon dispersion as $\omega_{n\mathbf{k}} = \bar{\omega} + \delta_{n\mathbf{k}}$, and retain the relevant temperature-dependent terms, so that

$$\sum_{n\mathbf{k}} \frac{A_{n\mathbf{k}}}{e^{\omega_{n\mathbf{k}}/k_B T} - 1} = \sum_{n\mathbf{k}} \frac{A_{n\mathbf{k}}}{e^{(\bar{\omega} + \delta_{n\mathbf{k}})/k_B T} - 1}, \quad (8)$$

where we have defined $A_{n\mathbf{k}} = a_{n\mathbf{k}}/\omega_{n\mathbf{k}}$. The Einstein approximation assumes that it is possible to find a $\bar{\omega}$ such that the variations in the dispersion $\delta_{n\mathbf{k}}$ can be neglected, leading to $A_0 = \sum_{n\mathbf{k}} A_{n\mathbf{k}}$. To go beyond the Einstein approximation, we expand deviations in $\omega_{n\mathbf{k}}$ from $\bar{\omega}$ in small $\delta_{n\mathbf{k}}/\bar{\omega} \ll 1$, giving

$$\begin{aligned} \sum_{n\mathbf{k}} \frac{A_{n\mathbf{k}}}{e^{\omega_{n\mathbf{k}}/k_B T} - 1} &= \frac{\sum_{n,\mathbf{k}} A_{n\mathbf{k}}}{e^{\bar{\omega}/k_B T} - 1} - \frac{e^{\bar{\omega}/k_B T} \sum_{n,\mathbf{k}} A_{n\mathbf{k}} \delta_{n\mathbf{k}}}{k_B T (e^{\bar{\omega}/k_B T} - 1)^2} \\ &+ \frac{e^{\bar{\omega}/k_B T} (1 + e^{\bar{\omega}/k_B T}) \sum_{n,\mathbf{k}} A_{n\mathbf{k}} \delta_{n\mathbf{k}}^2}{2(k_B T)^2 (e^{\bar{\omega}/k_B T} - 1)^3} \\ &+ \mathcal{O}(\delta_{n\mathbf{k}}^3). \end{aligned} \quad (9)$$

This form provides a systematic way of improving upon the BE oscillator model, at the expense of increasing the number of fitting parameters. The function we fit is shown in Table I with fitting parameters $\bar{\omega}$ and $A_i = \sum_{n,\mathbf{k}} A_{n\mathbf{k}} \delta_{n\mathbf{k}}^i$. We refer to this approach as the *ith-order phonon dispersion method*, where *i* refers to the highest order power of $\delta_{n\mathbf{k}}$ included. To determine the most appropriate order for the phonon dispersion method, the reduced- χ^2 test may be used.

2. Two-step method

The phonon dispersion expansion introduces extra fitting parameters compared to the BE oscillator model, which might make it difficult to perform an accurate fit and extrapolation with low-quality or sparse experimental data. We therefore propose an alternative method, based on fitting only the BE oscillator form to the experimental data, but requiring a recursive fit.

In general, the BE fit parameters \mathbf{A} will depend on the maximum temperature included in the fit $\mathbf{A} = \mathbf{A}(T_{\max})$. As shown in the Appendix, the high-temperature asymptotes for $\omega(T_{\max})$ and $A(T_{\max})$ in the BE oscillator

fit are

$$\omega(T_{\max}) = p_0 + \frac{p_1 p_0^2}{k_B T_{\max} \ln(p_0/k_B T_{\max})}, \quad (10)$$

$$A(T_{\max}) = p_2 \left(p_0 + \frac{p_1 p_0^2}{k_B T_{\max}} \right), \quad (11)$$

where p_0 , p_1 , and p_2 are fitting parameters. The underlying phonon dispersion can be extracted from these parameters following the prescription described in the Appendix. This motivates a scheme that can be implemented in two stages:

(1) Fit the single BE, Eq. (7), to the data for a range of maximum temperatures T_{\max} .

(2) Fit Eqs. (10) and (11) to the functions $\omega(T_{\max})$ and $A(T_{\max})$ obtained in stage 1.

The final ZP correction is then $p_2 p_0$. This scheme only requires fitting of the two-parameter BE oscillator model to the experimental data.

B. Benchmarking the extrapolation schemes

First-principles calculations of the temperature dependence of the thermal band gap of diamond and lithium hydride (LiH) [22] provide contrasting systems which we can use to test the relative merits and accuracy of our two models and the previous schemes. Diamond has a simple phonon dispersion, leading to a monotonic temperature dependence of the band gap, whereas LiH has widely separated acoustic and optical branches, leading to a more challenging nonmonotonic temperature dependence of the gap. The calculations were performed using plane-wave density functional theory [40,41] with ultrasoft pseudopotentials [42] as implemented in the CASTEP code [43]. We have used the local density approximation [44,45] to the exchange-correlation functional, an energy cutoff of 1000 eV, and a Monkhorst-Pack [46] \mathbf{k} -point grid of spacing $2\pi \times 0.04 \text{ \AA}^{-1}$.

1. Diamond

Diamond is an ideal test bed for the temperature dependence of band gaps because both first-principles results and experimental data are available. The upper part of Fig. 1 shows the temperature dependence of the band gap as given by Eq. (4) including 162 phonon modes (corresponding to a supercell with 54 atoms) and with the couplings calculated from first principles using the method described in Ref. [22]. The results of this calculation are in good agreement with experiment, and the first-principles calculation gives a ZP correction to the gap of -0.462 eV .

As first-principles data give the full temperature dependence of band gaps, we can use it to test how the range of data available determines the quality of the ZP extrapolation schemes of Table I. The extrapolated ZP corrections from a fit to the first-principles data recover the first-principles ZP correction if data at sufficiently high temperatures is included. Using one or two BE oscillators leads to reasonable fits allowing us to estimate the ZP correction. However, the convergence is slow, requiring data from temperatures up to about 3000 K to estimate the ZP correction within 0.01 eV. The Pässler form has more degrees of freedom than a single BE oscillator and, even though (depending on the temperature

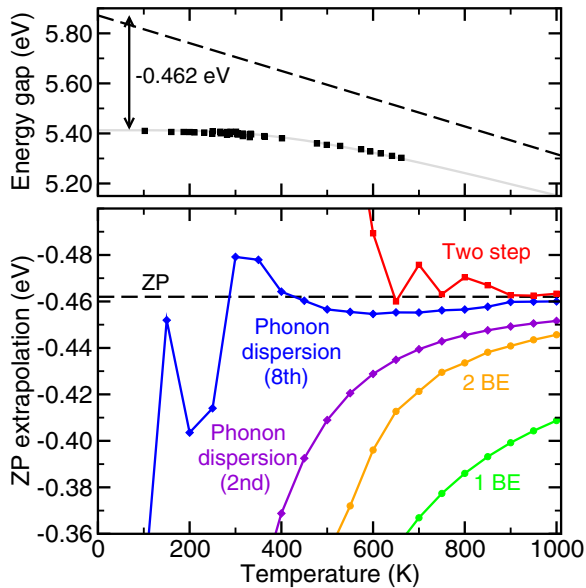


FIG. 1. (Color online) Upper: Temperature dependence of the thermal band gap of diamond. The experimental data (black squares, from Ref. [6]) are compared to the first-principles results (gray solid line) that have been shifted to match the experimental data at zero temperature. The high-temperature linear extrapolation is also shown (black dashed line). Lower: ZP correction to the thermal band gap of diamond obtained with the linear extrapolation scheme, using the most accurate models listed in Table I. The horizontal dashed line in the lower part of the figure labeled “ZP” denotes the value obtained from the first-principles calculations.

range) it leads to a fit with a smaller mean square deviation, the extrapolation to zero temperature leads to worse results than fits based on the BE oscillator, and the extrapolated values are outside of the range of Fig. 1. This can be explained by the emphasis of the Pässler form on the shape at low temperatures, which is not important for the asymptotic high-temperature limit or the ZP correction. The Varshni extrapolates lie outside of the plot limits.

The methods we have proposed lead to better estimates of the ZP correction. The phonon dispersion method with an expansion up to second order has the same number of fitting parameters as a double BE oscillator but consistently delivers better results. An expansion up to eighth order leads to results converged to better than 0.01 eV above 350 K. The two-step method outperforms all but the phonon dispersion method with an eighth-order expansion above 600 K, and leads to results comparable to the latter above 900 K.

Having established the limited applicability of standard extrapolation methods and proven the better performance of our two methods, we are well positioned to revisit the diamond experimental data discussed in Refs. [15,47]. The results from a variety of models to estimate the ZP correction are summarized in Table II. The phonon dispersion method used at fourth order is our benchmark for diamond. The single BE oscillator fit leads to poor results, in agreement with the theoretical assessment above. We also note that the BE oscillator extrapolation value reported in Ref. [47] disagrees with our value, which arises because we find different fit parameters. The two-step technique overestimates the value

TABLE II. ZP correction to the electronic band gap of diamond from the experimental data in Ref. [6].

	ZP correction (eV)
BE oscillator	-0.29
Two step	-0.51
4th-order phonon dispersion	-0.41
Isotope (Ref. [47])	-0.36

obtained by the phonon dispersion method, as also observed in our tests reported in Fig. 1. The isotope method described in Ref. [47] is an alternative approach for the determination of ZP band gap corrections based on experiments with different isotopes, and it is in fair agreement with the phonon dispersion method.

Having completed the analysis of the experimental data, it is instructive to compare the estimate for the ZP correction to that from our first-principles calculations. The phonon dispersion extrapolation scheme applied to the experimental data gives -0.41 eV, in reasonable agreement with the theoretical value of -0.46 eV.

2. Lithium hydride

The temperature dependence of the thermal band gap of LiH [22] provides a more challenging example for the extrapolation schemes. LiH is representative of a class of systems in which the acoustic and optical phonon branches present qualitatively different behavior, leading to a nonmonotonic temperature dependence of the band gap, as shown in Fig. 2. The effect of the low-energy acoustic phonons is to open the gap, while the high-energy optical phonons close the gap. The reduction in the gap due to the ZP correction is -0.084 eV. The gap initially opens with increasing temperature due to the

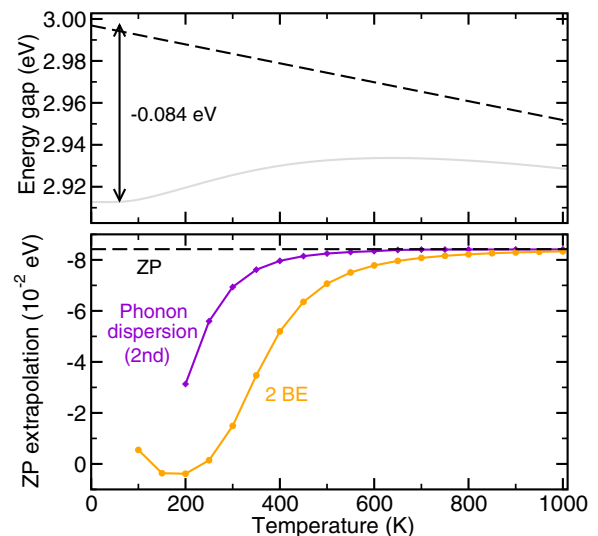


FIG. 2. (Color online) Upper: Temperature dependence of the thermal band gap of LiH. We show first-principles results (gray solid line) and the high-temperature linear extrapolation (black dashed line). Lower: ZP correction to the thermal band gap of LiH obtained with the linear extrapolation scheme, using the most accurate models listed in Table I. 2 BE denotes double BE.

thermal excitation of low-energy acoustic phonons. This trend is reversed at temperatures around $T = 700$ K, when higher energy optical phonons become thermally excited. Capturing the linear part of the temperature dependence requires data above the melting temperature of $T = 960$ K, motivating the exploration of more sophisticated extrapolation methods.

A single BE oscillator fails to describe a nonmonotonic temperature dependence, and when the system presents different characteristic frequencies for the low- and high-energy phonons, a double BE oscillator model is required [11]. In Fig. 2 we show the extrapolated ZP correction to the band gap of LiH using a double BE oscillator model. We also show the extrapolated ZP correction obtained from the most successful method of those proposed, the phonon dispersion method. With a second-order expansion the phonon dispersion method performs significantly better than a double BE oscillator. The two-step method works very well for diamond above a temperature of about $T = 600$ K, but it fails for the temperatures considered for LiH. We note that no experimental data are available for the temperature dependence of the band gap of LiH, and therefore our result stands as a prediction which will hopefully be tested against experiment in the future.

The use of an accurate method that delivers converged results with lower temperature data becomes crucial in LiH, whose melting temperature is $T = 960$ K. Both examples (diamond and LiH) show that the phonon dispersion method leads to an order-of-magnitude improvement compared to standard single or double BE oscillator fits. Therefore, we recommend the phonon dispersion method for extracting ZP corrections to electronic band gaps.

IV. LOW-TEMPERATURE FORMALISM

Low-dimensional systems such as graphene, molybdenum disulfide, hexagonal boron nitride, and carbon nanotubes, have enjoyed significant research interest over the last decade [48], and it is therefore important to study their temperature-dependent properties. The low-temperature behavior is difficult to obtain from numerical simulations, so it is instead important to derive analytical expressions. In this section we review the asymptotic behavior [36] at low temperatures in 3-dimensional solids, and extend it for the first time, as far as we are aware, to low-dimensional systems. At low temperatures, only the lowest energy acoustic modes are excited, so these modes must be treated explicitly.

A. Three-dimensional T^4 power law

We first consider the three-dimensional system, where our derivation follows closely that in Ref. [49] for the specific heat. In the limit of a large solid, the \mathbf{k} points become dense on the length scale over which physical quantities vary appreciably. This allows us to replace summations over \mathbf{k} by integrals over the first BZ of volume V_{BZ} in Eq. (4),

$$\langle \hat{O} \rangle = \sum_n \int_{\text{BZ}} \frac{d^3\mathbf{k}}{(2\pi)^3 V_{\text{BZ}}} \frac{a_n(\mathbf{k})}{2\omega_n(\mathbf{k})} [1 + 2n_{\text{B}}(\omega_n(\mathbf{k}))], \quad (12)$$

where the sum is over the n phonon branches. The BE factor forces the occupancies of the modes with energies $\omega_n(\mathbf{k}) \gg k_{\text{B}}T$ to vanish exponentially with decreasing temperature, and

therefore only the three acoustic modes $\omega_n(\mathbf{k}) = c_n(\hat{\mathbf{k}})|\mathbf{k}|$ for which $\omega_n(\mathbf{k}) \rightarrow 0$ as $|\mathbf{k}| \rightarrow 0$ contribute as $T \rightarrow 0$. The acoustic modes dominate within the BZ but vanish exponentially outside of it. We can therefore expand the range of the integral to the entire \mathbf{k} space and, as only the neighborhood of the Γ point contributes to the integral, we can expand the couplings $a_n(\mathbf{k})$ in small $\omega_n(\mathbf{k})$ as $a_n(\mathbf{k}) \simeq a_n^{(2)}[c_n(\hat{\mathbf{k}})|\mathbf{k}|]^2$. This expansion uses the fact that $a_n(\mathbf{0}) = 0$ at $\mathbf{k} = \mathbf{0}$ (to enforce translational invariance), and the linear term vanishes for the band gap [36]. The expectation value then reads

$$\langle \hat{O} \rangle = \frac{3a}{2\pi^2 c^3} (k_{\text{B}}T)^2 \int_0^\infty dx x^3 n_{\text{B}}(x) = \frac{3\Gamma(4)\zeta(4)a}{2\pi^2 c^3} (k_{\text{B}}T)^4, \quad (13)$$

where $a/c^3 = \frac{1}{3V_{\text{BZ}}} \sum_n a_n^{(2)} \int \frac{d\Omega}{4\pi} c_n(\hat{\mathbf{k}})^{-3}$ and $d\Omega$ is the infinitesimal angular element. $\Gamma(p+2) = (p+1)!$ is the gamma function for integer p , and ζ is the Riemann zeta function. We therefore recover the power law of Ref. [36],

$$\langle \hat{O} \rangle = \frac{\pi^2 a}{10c^3} (k_{\text{B}}T)^4, \quad (14)$$

with a prefactor that depends on the parameter a/c^3 , that can be determined by fitting to experimental data.

We note that this result is valid for the class of observables (including the band gap) for which $a_n(\mathbf{k})$ has a quadratic dependence on the energy around $\mathbf{k} = \mathbf{0}$ [36]. However, the methodology presented here is more general, so it could be applied to other classes of observables with different asymptotic behavior.

B. Low-dimensional systems

In this section we extend the low-temperature results to 2- and 1-dimensional systems. Low-dimensional systems are important in understanding exotic physical properties and for technological applications. Low-dimensional systems are qualitatively different from 3-dimensional systems because linear and quadratic acoustic branches coexist. This qualitatively different behavior makes a detailed study of the low-dimensional systems essential.

In a 2-dimensional system, there are two acoustic branches with linear dispersion, and the other with quadratic dispersion corresponding to out-of-plane atomic motion. A 1-dimensional system has a single acoustic linear branch and two quadratic acoustic branches.

For 2- and 1-dimensional systems the linear branches lead to

$$\langle \hat{O} \rangle_{\text{2D}}^{\text{linear}} = \frac{2\zeta(3)a}{\pi c^2} (k_{\text{B}}T)^3, \quad (15)$$

$$\langle \hat{O} \rangle_{\text{1D}}^{\text{linear}} = \frac{\zeta(2)a}{2\pi c} (k_{\text{B}}T)^2. \quad (16)$$

The quadratic branches with $\omega_n(\mathbf{k}) = c_n(\hat{\mathbf{k}})k^2$ lead to

$$\langle \hat{O} \rangle_{\text{2D}}^{\text{quadratic}} = \frac{\pi a}{24c^2} (k_{\text{B}}T)^2, \quad (17)$$

$$\langle \hat{O} \rangle_{\text{1D}}^{\text{quadratic}} = \frac{a}{8(\pi c)^{1/2}} \zeta\left(\frac{3}{2}\right) (k_{\text{B}}T)^{3/2}. \quad (18)$$

The low-temperature asymptote of the lower-dimensional systems is dominated by the quadratic phonon branches.

A finite (0-dimensional) system has discrete phonon modes. Hence, the temperature dependence as $T \rightarrow 0$ is a discrete sum of BE oscillators with an asymptotic exponential behavior.

V. CONCLUSIONS

We have studied extrapolation schemes for estimating the ZP correction of phonon-dependent properties from knowledge of their temperature dependence. We have shown that standard schemes fail to recover the correct asymptotic limit, and therefore proposed and tested two strategies that deliver results of higher accuracy. The application of our schemes to diamond has allowed us to extract a more accurate value for the ZP correction to the band gap from experimental data. We have also tested them on lithium hydride, which presents a band gap with a nonmonotonic temperature dependence. Based on our results, we recommend the dispersion method for the extraction of ZP corrections to band gaps from experimental data.

The extraction of ZP corrections to electronic band gaps is becoming increasingly important. Recent interest in first-principles calculations of the temperature dependence of band gaps calls for accurate experimental data for a wide variety of materials. We believe that the proposed method will contribute in bridging the gap between theory and experiment in this area. Furthermore, similar behavior is observed in the temperature dependence of other physical properties, such as thermal expansion or the chemical shielding tensor, and therefore the ideas described in this work could be extended to a wider range of properties.

We have also discussed the properties of the temperature dependence of band gaps in the limit $T \rightarrow 0$, recovering the standard T^4 power law for three-dimensional solids, and obtaining a T^2 power law in two dimensions and a $T^{3/2}$ power law in one dimension.

ACKNOWLEDGMENTS

B.M. and R.J.N. acknowledge the financial support of the Engineering and Physical Sciences Research Council (UK), and G.J.C. funding from Gonville & Caius College, and a Samsung GRO.

APPENDIX: ASYMPTOTIC TEMPERATURE DEPENDENCE

Here we present the derivation of Eqs. (10) and (11). We perform a least-squares fit of the Bose-Einstein oscillator model to the data described by Eq. (4). The square deviation

of the model compared with the data is

$$\langle \Delta^2 \rangle = \int_{\infty}^{\beta_{\max}} \left(\underbrace{\frac{A}{e^{\beta\omega} - 1} - \sum_{n,\mathbf{k}} \frac{A_{n\mathbf{k}}}{e^{\beta\omega_{n\mathbf{k}}} - 1}}_{F(\beta,A,\omega)} \right)^2 J(\beta) d\beta, \quad (\text{A1})$$

where we have retained the terms relevant for the temperature dependence, $J(\beta) = \beta^{-2}$ is the Jacobian, and $\beta_{\max} = 1/k_B T_{\max}$ is the maximum temperature of the data included in the fit.

The fitting parameters (A, ω) depend on β_{\max} . We take a small β_{\max} (high temperature) expansion of Eqs. (10) and (11), and the parameters (A, ω) should obey

$$\begin{aligned} \frac{\partial \langle \Delta^2 \rangle}{\partial A} &= 2 \int_{\infty}^{\beta_{\max}} \left(\frac{1}{\beta\omega} - \frac{1}{2} + \mathcal{O}(\beta) \right) F(\beta, A, \omega) J(\beta) d\beta = 0, \\ \frac{\partial \langle \Delta^2 \rangle}{\partial \omega} &= 2A \int_{\infty}^{\beta_{\max}} \left(\frac{1}{\beta\omega^2} + \mathcal{O}(\beta) \right) F(\beta, A, \omega) J(\beta) d\beta = 0. \end{aligned} \quad (\text{A2})$$

The β dependence of the first term in the expansion is the same in both equations. For small β we may neglect terms linear in β . After evaluating the integrals, we obtain two equations

$$\begin{aligned} A \left[-\beta_{\max} + \frac{1}{\omega} \ln(e^{\beta_{\max}\omega} - 1) \right] - \left[-\beta_{\max} \sum_{n,\mathbf{k}} A_{n\mathbf{k}} \right. \\ \left. + \sum_{n,\mathbf{k}} \frac{A_{n\mathbf{k}}}{\omega_{n\mathbf{k}}} \ln(e^{\beta_{\max}\omega_{n\mathbf{k}}} - 1) \right] = 0, \end{aligned} \quad (\text{A3})$$

$$\frac{A}{\omega^2} \text{Li}_2(e^{-\beta_{\max}\omega}) - \sum_{n,\mathbf{k}} \frac{A_{n\mathbf{k}}}{\omega_{n\mathbf{k}}^2} \text{Li}_2(e^{-\beta_{\max}\omega_{n\mathbf{k}}}) = 0, \quad (\text{A4})$$

where Li_2 is a polylogarithm of order 2. This system of equations can be solved algebraically by means of the Newton-Raphson method in the high-temperature limit to yield, to lowest order,

$$\begin{aligned} \omega(\beta_{\max}) &= \frac{g_{-1}}{g_{-2}} - \frac{6\beta_{\max} \ln \frac{g_{-1}}{g_{-2}\Omega} g_{-1}^2}{\pi^2 \ln \frac{\beta_{\max} g_{-1}}{g_{-2}} g_{-2}^2}, \\ A(\beta_{\max}) &= \frac{g_{-1}^2}{g_{-2}} - \frac{6\beta_{\max} \ln \frac{g_{-1}}{g_{-2}\Omega} g_{-1}^3}{\pi^2 g_{-2}^2}, \end{aligned} \quad (\text{A5})$$

where $g_{-1} = \sum_{n\mathbf{k}} A_{n\mathbf{k}} \omega_{n\mathbf{k}}^{-1}$, $g_{-2} = \sum_{n\mathbf{k}} A_{n\mathbf{k}} \omega_{n\mathbf{k}}^{-2}$, and $\ln \Omega = g_{-1}^{-1} \sum_{n\mathbf{k}} A_{n\mathbf{k}} \omega_{n\mathbf{k}}^{-1} \ln \omega_{n\mathbf{k}}$, and we have retained only the lowest order terms for each power. This recovers the lowest order terms for the ω dependence in Eq. (10) and the A dependence in Eq. (11).

In terms of the fitting parameters in Eqs. (10) and (11), we have $p_0 = \frac{g_{-1}}{g_{-2}}$, $p_1 = \frac{6}{\pi^2} \ln \frac{g_{-1}}{g_{-2}\Omega}$, and $p_2 = g_{-1}$.

[1] A. Einstein, *Ann. Phys.* **327**, 180 (1906).

[2] P. Debye, *Ann. Phys.* **344**, 789 (1912).

[3] P. Giannozzi, S. de Gironcoli, P. Pavone, and S. Baroni, *Phys. Rev. B* **43**, 7231 (1991).

- [4] S. Baroni, S. de Gironcoli, A. Dal Corso, and P. Giannozzi, *Rev. Mod. Phys.* **73**, 515 (2001).
- [5] H. Fesefeldt, *Z. Phys.* **64**, 623 (1930).
- [6] C. D. Clark, P. J. Dean, and P. V. Harris, *Proc. R. Soc. London, Ser. A* **277**, 312 (1964).
- [7] W. Choyke, in *Silicon Carbide—1968*, edited by H. Hensch and R. Roy (Pergamon, New York, 1969), pp. S141–S152.
- [8] W. Bludau, A. Onton, and W. Heinke, *J. Appl. Phys.* **45**, 1846 (1974).
- [9] S. Logothetidis, J. Petalas, H. M. Polatoglou, and D. Fuchs, *Phys. Rev. B* **46**, 4483 (1992).
- [10] L. Artus and Y. Bertrand, *Solid State Commun.* **61**, 733 (1987).
- [11] J. Bhosale, A. K. Ramdas, A. Burger, A. Muñoz, A. H. Romero, M. Cardona, R. Lauck, and R. K. Kremer, *Phys. Rev. B* **86**, 195208 (2012).
- [12] X. Li, M. Han, X. Zhang, C. Shan, Z. Hu, Z. Zhu, and J. Chu, *Phys. Rev. B* **90**, 035308 (2014).
- [13] P. B. Allen and V. Heine, *J. Phys. C* **9**, 2305 (1976).
- [14] P. B. Allen and M. Cardona, *Phys. Rev. B* **23**, 1495 (1981).
- [15] M. Cardona and M. L. W. Thewalt, *Rev. Mod. Phys.* **77**, 1173 (2005).
- [16] R. D. King-Smith, R. J. Needs, V. Heine, and M. J. Hodgson, *Europhys. Lett.* **10**, 569 (1989).
- [17] R. B. Capaz, C. D. Spataru, P. Tangney, M. L. Cohen, and S. G. Louie, *Phys. Rev. Lett.* **94**, 036801 (2005).
- [18] F. Giustino, S. G. Louie, and M. L. Cohen, *Phys. Rev. Lett.* **105**, 265501 (2010).
- [19] X. Gonze, P. Boulanger, and M. Côté, *Ann. Phys.* **523**, 168 (2011).
- [20] E. Cannuccia and A. Marini, *Phys. Rev. Lett.* **107**, 255501 (2011).
- [21] E. Cannuccia and A. Marini, *Eur. Phys. J. B* **85**, 320 (2012).
- [22] B. Monserrat, N. D. Drummond, and R. J. Needs, *Phys. Rev. B* **87**, 144302 (2013).
- [23] C. E. Patrick and F. Giustino, *Nat. Commun.* **4**, 2006 (2013).
- [24] P. Han and G. Bester, *Phys. Rev. B* **88**, 165311 (2013).
- [25] S. Poncé, G. Antonius, P. Boulanger, E. Cannuccia, A. Marini, M. Côté, and X. Gonze, *Comput. Mater. Sci.* **83**, 341 (2014).
- [26] B. Monserrat, N. D. Drummond, C. J. Pickard, and R. J. Needs, *Phys. Rev. Lett.* **112**, 055504 (2014).
- [27] G. Antonius, S. Poncé, P. Boulanger, M. Côté, and X. Gonze, *Phys. Rev. Lett.* **112**, 215501 (2014).
- [28] B. Monserrat and R. J. Needs, *Phys. Rev. B* **89**, 214304 (2014).
- [29] C. E. Patrick and F. Giustino, *J. Phys. Condens. Matter* **26**, 365503 (2014).
- [30] I. Garate, *Phys. Rev. Lett.* **110**, 046402 (2013).
- [31] K. Saha and I. Garate, *Phys. Rev. B* **89**, 205103 (2014).
- [32] Y. Varshni, *Physica* **34**, 149 (1967).
- [33] A. Manoogian and A. Leclerc, *Can. J. Phys.* **57**, 1766 (1979).
- [34] L. Viña, S. Logothetidis, and M. Cardona, *Phys. Rev. B* **30**, 1979 (1984).
- [35] R. Pässler, *Phys. Status Solidi B* **236**, 710 (2003).
- [36] M. Cardona, T. A. Meyer, and M. L. W. Thewalt, *Phys. Rev. Lett.* **92**, 196403 (2004).
- [37] R. Ramírez, C. P. Herrero, and E. R. Hernández, *Phys. Rev. B* **73**, 245202 (2006).
- [38] M. A. Morales, J. M. McMahon, C. Pierleoni, and D. M. Ceperley, *Phys. Rev. B* **87**, 184107 (2013).
- [39] P. B. Allen, *Philos. Mag. B* **70**, 527 (1994).
- [40] P. Hohenberg and W. Kohn, *Phys. Rev.* **136**, B864 (1964).
- [41] W. Kohn and L. J. Sham, *Phys. Rev.* **140**, A1133 (1965).
- [42] D. Vanderbilt, *Phys. Rev. B* **41**, 7892 (1990).
- [43] S. J. Clark, M. D. Segall, C. J. Pickard, P. J. Hasnip, M. I. J. Probert, K. Refson, and M. C. Payne, *Z. Kristallogr.* **220**, 567 (2009).
- [44] D. M. Ceperley and B. J. Alder, *Phys. Rev. Lett.* **45**, 566 (1980).
- [45] J. P. Perdew and A. Zunger, *Phys. Rev. B* **23**, 5048 (1981).
- [46] H. J. Monkhorst and J. D. Pack, *Phys. Rev. B* **13**, 5188 (1976).
- [47] M. Cardona, *Solid State Commun.* **133**, 3 (2005).
- [48] A. K. Geim and K. S. Novoselov, *Nat. Mater.* **6**, 183 (2007).
- [49] N. W. Ashcroft and N. D. Mermin, *Solid State Physics* (Brooks/Cole Cengage Learning, Belmont, 1976).